Growth of AlGaN Film on Si (111) Substrate

Yang Zhang[1,2], Bingzhen Chen[2], Na Peng[2], Lu Zhang[2], Cuibai Yang[2], Xu Pan[2], Shun Yao[1], Zhiyong Wang[1]

[1]*Institute of Laser Engineering, Beijing University of Technology, Beijing 100022, China*

[2]*Guangdong redsolar photovoltaic technology Co.,LTD zhongshan528437,Guangdong , China*

Abstract: At present, the applications of $Al_xGa_{1-x}N$ are extensive, such as for visible-blind ultraviolet detectors, laser diodes, light emitting diodes (LEDs) and HEMTs**.** In this paper, $Al_{0.25}Ga_{0.75}N$ and $Al_{0.32}Ga_{0.68}N$ films have been grown on 2 in Si (111) substrates by MOCVD. The low-temperature (6 K) photoluminescence (PL) spectrum and XRD rocking curve measurements have been employed to study the crystal quality of samples, and the phonon replica peak can be observed, which indicate that the samples have better quality in a small-localized region. The surface morphology of samples was investigated by AFM and the result of wavy surface agrees with the deduction from XRD rocking curve measurements. The sheet resistance mappings have been shown, and it indicates the nonuniformity of AlGaN film on Si (111) will increase sharply as the Al content increases.

1. Introduction

GaN and related Group-III nitrides grown by metal-organic chemical-vapor deposition(MOCVD)can be applied to high power, high frequency and high-temperature electronic devices[1-3] as well as light emitting diodes (LEDs) and laser diodes. Ternary AlGaN in particular is an important one with wide direct band gap, which has a broad range of applications in ultraviolet (UV) optoelectronic devices[4-6]. Due to the limited availability of bulk GaN or AlN substrates for homoepitaxial growth, Generally GaN is grown on sapphire, SiC and Si substrates. The improvement of the power density of the device is limited by Sapphire substrate's bad thermal conduction. Meanwhile, the high cost of SiC substrates hinders the application of GaN material grown on SiC. Compared with sapphire and SiC, Si is the best alternative for its low cost, good thermal conductivity and ability to be integrated with the mature Si-based processing techniques[7, 8]. However, for the large lattice mismatch and the large coefficient of thermal-expansion (CTE) mismatch between GaN (AlN) and Si, the growth of high quality, thick crack-free AlGaN on Si substrate is a difficult task, and the cracks and high defect density seriously degrade the performance of GaN based devices on Si substrates. There are few reports on AlGaN growth on silicon substrates[9-11]. In this study, the epitaxy of AlGaN on 2 in Si (1 11) substrates was performed in a horizontal MOCVD reactor. The low-temperature (6K) photoluminescence (PL) spectrum and XRD rocking curve measurements have been employed to study the crystal quality of samples. We also investigate the surface morphology of AlGaN epilayers on Si (111) substrate by AFM. The sheet resistance mappings of samples indicate the nonuniformity of AlGaN film on Si (111) will increase sharply as the Al content increases.

2. Experiment

AlxGa1-xN epilayers were grown by MOCVD on 2-in Si (111) substrates. The Si substrates were degreased by hot H2SO4 solutions for 5 min, NH3•H2O:H2O2:H2O (1:1:5) solutions for 5 min, HCl: H2O2:H2O (1:1:5) solutions for 5 min in due order, and then etched with HF (2%) for 0.5 min to remove the surface oxide layer. This procedure results in an oxide-free, hydrogen-terminated Si surface. Trimethylaluminum (TMA), Trimethylgallium

(TMG), and ammonia were used as Al, Ga, and N sources, respectively. H2 was used as a carrier gas. After preparation, Si (111) substrates were heated under H2 ambient at 1060 ℃ for 3 min to clean its surface prior to growth. Pre-deposition of Al was used to prevent the formation of SiNx. In the initial stage of growth, a 60nm thick HT-AlN layer was grown, which is used as nucleation layer, and then 20 periods of AlN/GaN (2nm/3nm) superlattices was grown. The introduction of such superlattices aims at creating an additional compressive strain during the growth or the cooling down of the sample, in order to counterbalance the tensile strain in nitrides deposited on silicon[12]. Finally, another 30-40nm HT-AlN buffer layer was grown. Following the composite buffer layer, 500 nm Al0.25Ga0.75N epilayers and 500 nm Al0.32Ga0.68N epilayers were grown for sample A and B respectively. The samples were investigated by AFM and XRD rocking curve measurements. UV PL was performed in a home-made vacuum spectroscope. The excitation source was a frequency quadrupled Ti: sapphire laser. The sheet resistance mappings of samples were measured by LEI 1500 series contactless resistance mapping system.

3. Results and Discussion

The HR-XRD 2θ-ω scan for the sample has been measured. Using Vegard's law, the Al content in the AlxGa1-xN film can be estimated to be 25% and 32% respectively. The low-temperature (6 K) continuous-wave (cw) PL spectrum of samples is presented in Fig.1.

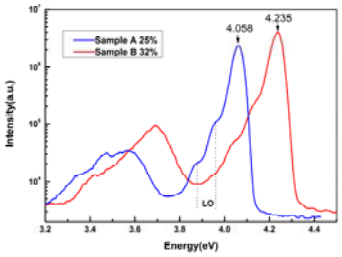

Fig.1. the low-temperature (6 K) continuous-wave(cw) PL spectrum of samples

It exhibits the main free excition emission line at 4.058 ev and 4.235 ev respectively. And the value of content deduced by band gap is in accordance with XRD's. Two weaker peaks are observed at each curve. The energy separation between the successive emission lines is about 90 mev [13-15], which corresponds to the value of the LO phonon energy in GaN. Thus, we assign the two lower energy peaks to the n=1 and n=2 phonon replicas of the main exciton transition line (n=0) in order by decreasing energy. The appearance of the phonon replica lines is a clear indicator of a strong carrier-phonon interaction in AlGaN on Si.

Under the optical microscope, many pits are observed on the surface of samples, especially in sample B. As we know, (Al)GaN epilayers on Si is a mosaic structure, several reports have indicated that the surface pits are attached to threading dislocations with screw components [16, 17] and the distribution is due to the misorientation between adjacent subgrains. We known at the same time that the full width of half maximum (FWHM) of the XRD rocking curve symmetric (0002) ω-scan is only broadened by dislocations consisting of screw components, therefore, for further studying the influence of the pits on crystal quality, the rocking curve symmetric (0002) ω-scan of our samples have been done, as shown in Fig.2 (a). A GaN epilayers sample with the same buffer structure also has been measured as a contrast. There is a visible bulge on low angle side for AlGaN samples. In combination with XRD schematic diagram, as shown in Fig.2 (b), the symmetry of curve shape is decided by the arrangement of crystal face which can satisfy a demand of Bragg reflection for X-ray.

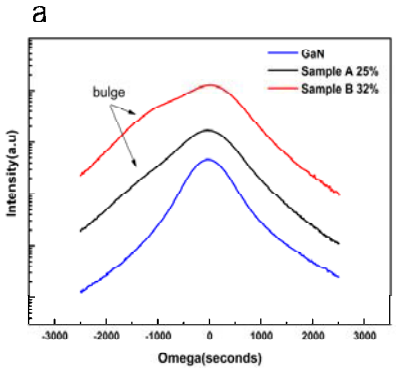

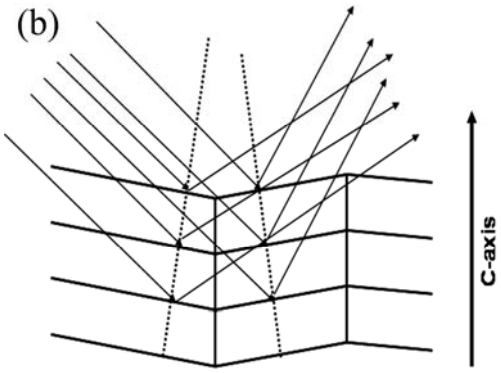

Fig.2. the rocking curve symmetric (0002) ω-scan of samples (a) and the schematic diagram of bulge appearance (b)

Thus, the result that sample B has a larger bulge implies that the film preferred orientation (001) represents a more deviation compared with sample A. The appearance of a large number of pits is a good evidence for the deviation of orientation (001) between adjacent subgrains. In fact, AFM measurements also agree with the deduction from XRD rocking curve measurements. As shown in Fig.3; the root-mean-square (rms) roughness is 3.69 nm for sample A and 5.23 nm for sample B in 5×5μm2 scan area, and pits scatter on the two sample's surface.

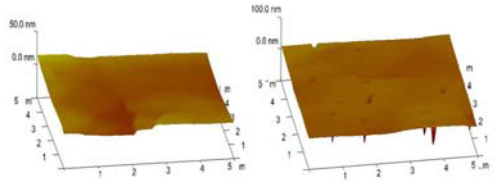

Fig.3. 3D AFM images (5×5μm2 scan) of Al0.25Ga0.75N (left) and Al0.32Ga0.68N (right)

Besides the pits, the wavy surface is also observed as shown in the set of Fig.3. The stepping curve is the white line trace in AFM measurements. The wavy surface has a low density of pits and the flat surface has a high density of pits. Taking AlGaN/Si, the big mismatch system into consideration, the probable interpretation is that the formation of the wavy surface is a way to accommodate strain energy and the formation of pits is a way to release the tensile pressure, which is all caused by CTE or lattice mismatch between AlGaN and Si. When the Al content reaches the threshold value, may be 30%, the function of accommodation will switch to stress release and led finally to the formation of pits. In addition, the sheet resistance mappings of the samples are shown in Fig.4,

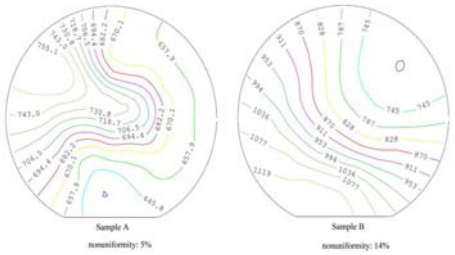

Fig.4. the sheet resistance mappings of samples

Obviously, the nonuniformity increases sharply as the Al content increases. Although the 5% nonuniformity of sample A is just passable, the value can still be reduced for preparation of devices.

4. Conclusion

AlGaN film has been grown on Si (111) substrates. The low-temperature PL spectrum shows two clear phonon replica peaks which indicate the samples have better quality in a small-localized region. The film preferred orientation (001) represents a deviation by analysis of XRD rocking curve. AFM measurements show two type of surface morphology, further analysis indicate that there may be a critical Al content value for the formation of surface pits. In addition, the wafer nonuniformity increases sharply as the Al content increases.

References

1. M.A. Khan, M.S. Shur, J.N. Kuznia, Q. Chen, J. Burm, W. Schaff, Temperature Activated Conductance in Gan/Algan Heterostructure Field-Effect Transistors Operating at Temperatures up to 300-Degrees-C, Appl Phys Lett, **66** (1995) 1083-1085.
2. S. Yoshida, J. Suzuki, Reliability of metal semiconductor field-effect transistor using GaN at high temperature, J Appl Phys, **84** (1998) 2940-2942.
3. 3.O. Aktas, Z.F. Fan, S.N. Mohammad, A.E. Botchkarev, H. Morkoc, High temperature characteristics of AlGaN/GaN modulation doped field-effect transistors, Appl Phys Lett, **69** (1996) 3872-3874.
4. V. Adivarahan, W.H. Sun, A. Chitnis, M. Shatalov, S.

Wu, H.P. Maruska, M.A. Khan, 250 nm AlGaN light-emitting diodes, Appl Phys Lett, **85** (2004) 2175-2177.

5. R. McClintock, A. Yasan, K. Mayes, D. Shiell, S.R. Darvish, P. Kung, M. Razeghi, High quantum efficiency AlGaN solar-blind p-i-n photodiodes, Appl Phys Lett, **84**(2004) 1248-1250.
6. J.Y. Duboz, N. Grandjean, F. Omnes, J.L. Reverchon, M. Mosca, Solar blind detectors based on AlGaN grown on sapphire, E-MRS 2004 Fall Meeting Symposia C and F, **2** (2005) 964-971.
7. A. Dadgar, M. Poschenrieder, J. Blasing, O. Contreras, F. Bertram, T. Riemann, A. Reiher, M. Kunze, I. Daumiller, A. Krtschil, A. Diez, A. Kaluza, A. Modlich, M. Kamp, J. Christen, F.A. Ponce, E. Kohn, A. Krost, MOVPE growth of GaN on Si(111) substrates, J Cryst Growth, **248** (2003) 556-562.
8. G.Y. Zhao, H. Ishikawa, H. Jiang, T. Egawa, T. Jimbo, M. Umeno, Optical absorption and photoluminescence studies of n-type GaN, Jpn J Appl Phys 2, **38** (1999) L993-L995.
9. S. Nikishin, G. Kipshidze, V. Kuryatkov, K. Choi, I. Gherasoiu, L.G. de Peralta, A. Zubrilov, V. Tretyakov, K. Copeland, T. Prokofyeva, M. Holtz, R. Asomoza, Y. Kudryavtsev, H. Temkin, Gas source molecular beam epitaxy of high quality AlxGa1-xN (0 <= x <= 1) on Si(111), Journal of Vacuum Science & Technology B-an International Journal Devoted to Microelectronics and Nanometer Structures-Processing Measurement and Phenomena, **19** (2001) 1409-1412.
10. M.A. Sanchez-Garcia, E. Calleja, F.B. Naranjo, F.J. Sanchez, F. Calle, E. Munoz, A.M. Sanchez, F.J. Pacheco, S.I. Molina, MBE growth of GaN and AlGaN layers on Si(111) substrates: doping effects, J Cryst Growth, **202** (1999) 415-418.
11. K. Cheng, M. Leys, J. Derluyn, K. Balachander, S. Degroote, M. Germain, G. Borghs, AlGaN-based heterostructures grown on 4 inch Si(111) by MOVPE, Physica Status Solidi C - Current Topics in Solid State Physics, Vol 5, No 6, **5** (2008) 1600-1602.
12. E. Feltin, B. Beaumont, M. Laugt, P. de Mierry, P. Vennegues, H. Lahreche, M. Leroux, P. Gibart, Stress control in GaN grown on silicon (111) by metalorganic vapor phase epitaxy, Appl Phys Lett, **79** (2001) 3230-3232.
13. W. Liu, M.F. Li, S.J. Xu, K. Uchida, K. Matsumoto, Phonon-assisted photoluminescence in wurtzite GaN epilayer, Semicond Sci Tech, **13** (1998) 769-772.
14. A. Sedhain, J. Li, J.Y. Lin, H.X. Jiang, Probing exciton-phonon interaction in AlN epilayers by photoluminescence, Appl Phys Lett, **95** (2009).
15. L. Bergman, M. Dutta, C. Balkas, R.F. Davis, J.A. Christman, D. Alexson, R.J. Nemanich, Raman analysis of the E1 and A1 quasi-longitudinal optical and quasi-transverse optical modes in wurtzite AlN, J Appl Phys, **85** (1999) 3535-3539.
16. B. Jahnen, M. Albrecht, W. Dorsch, S. Christiansen, H.P. Strunk, D. Hanser, R.F. Davis, Pinholes, dislocations and strain relaxation in InGaN, Mrs Internet J N S R, **3** (1998) art. no.-39.
17. H. Sasaki, S. Kato, T. Matsuda, Y. Sato, M. Iwami, S. Yoshida, Investigation of surface defect structure originating in dislocations in AlGaN/GaN epitaxial layer grown on a Si substrate, J Cryst Growth, **298**(2007) 305-309.